



Horizon 2020  
European Union Funding  
for Research & Innovation

# REPORT

---

## Developments in Topology Optimization in the ADDMAN Project

Henrik Alm Grundström

LIU-IEI-WP--18/00009—SE



## 1. Introduction

This document gives an account of some of the work done so far on topology optimization (TO) in the ADDMAN project. As well as the mathematical formulations and implementations details, short discussions are presented on some of the nuances of the different formulations and how they should be used efficiently.

## 2. Stress Constraints

The implementation of stress constraints in Trinitas is based on the work of Le et. al. and Holmberg et. al. [1] [2]. This section gives a short description of the stress relaxation, aggregation, clustering and correction currently implemented and available in Trinitas. The sensitivities for general equivalent stress constraints is derived with specific expressions for the von Mises equivalent stress and the maximum principle stress.

### 2.1 Constraint Relaxation

In order to avoid large stresses in areas of void the stress constraints are relaxed using the  $qp$ -relaxation as described in [3],

$$\sigma_a = C b_a u_e \rho_e^q \quad (2.1)$$

where  $\sigma_a$  is the stress state in Gauss point  $a$  of element  $e$ ,  $C$  is the constitutive matrix,  $b_a$  is the strain-displacement matrix for Gauss point  $a$  of element  $e$ ,  $u_e$  is the displacement vector for element  $e$ ,  $\rho_e$  is the physical design variable associated to element  $e$  and  $q$  is the penalization exponent usually set to  $q = 0.5$  (with  $p = 3$ ).

### 2.2 Constraint Aggregation and Clustering

Since the stresses are evaluated in each Gauss point of every element, the number of constraints necessary to enforce a stress limit in every point makes the problem computationally expensive. In order to circumvent this a stress aggregation function is used to approximate the maximum stress in the structure. Depending on the type of clustering technique used the maximum stress is approximated using either the  $P$ -norm function

$$\tilde{\sigma}_i^{Pn} = \left( \sum_{a=1}^{n_{a,i}} \tilde{\sigma}_a^P \right)^{\frac{1}{P}}, i = 1, \dots, n_c, \quad (2.2)$$

or the  $P$ -mean function

$$\tilde{\sigma}_i^{Pm} = \left( \frac{1}{n_{a,i}} \sum_{a=1}^{n_{a,i}} \tilde{\sigma}_a^P \right)^{\frac{1}{P}}, i = 1, \dots, n_c, \quad (2.3)$$

where  $\tilde{\sigma}$  is an equivalent stress measure (either the von-Mises stress or the largest (most positive) principle stress),  $n_{a,i}$  is the number of stress evaluation points in cluster  $i$  and  $n_c$  is the number of clusters. The  $P$ -norm overestimates the largest stress while the  $P$ -mean underestimates it, none is especially accurate. For  $P$  values in the range 8-24, the error in the estimation of the largest stress is typically around 15-25%. This error can be reduced significantly by using a stress correction factor as described in Section 2.3.

Three different clustering techniques are implemented in Trinitas; “element numbers”, which is basically an arbitrary partitioning of the stress evaluation points based on the element numbering, “stress level”, where elements with similar stress levels are grouped and “distributed stress”, where the elements with the largest stresses are placed in different clusters.

As an example consider the following:

$$\sigma_1 > \sigma_2 > \dots > \sigma_n.$$

If  $m$  “stress level” clusters are used, the first cluster would be

$$c_1^{sl} = \{\sigma_1, \sigma_2, \sigma_3, \dots\}.$$

If  $m$  “distributed stress” clusters are used, the first cluster would be

$$c_1^{ds} = \{\sigma_1, \sigma_{m+1}, \sigma_{2m+1}, \dots\}.$$

Since the stress levels change during the optimization iterations a “reclustering frequency”  $f_c$  can be specified in order to redo the clustering at a specified frequency. If  $I$  is the iteration counter, the reclustering is performed when  $I/f_c \in \mathbb{Z}$ . For large models with many loadcases the reclustering can be computationally expensive, therefor a parallel sorting algorithm is used for this task [4]. If the “element numbers” clusters are used, the reclustering has no effect.

The  $P$ -norm stress aggregation is used for the “element numbers” and “distributed stress” clustering methods and the  $P$ -mean is used for “stress level” clusters. The motivation for this is that the  $P$ -mean is more accurate when the stresses in the cluster are similar. If all the stresses are the same, the  $P$ -mean would be exact [2].

## 2.3 Stress Correction

The accuracy of the  $P$ -norm and  $P$ -mean stress aggregation functions is quite poor for any reasonable choice of  $P$ . However, since the actual largest stress in any cluster is easily obtainable, a correction factor can be calculated such that the aggregation function becomes exact. This correction factor is of course different in each iteration, therefore a damping factor is used to stop it from changing too much between iterations. The stress correction factor(s)  $c_i^I$  is calculated as follows

$$c_i^I = \alpha \frac{\tilde{\sigma}_{i,max}^I}{\tilde{\sigma}_i^{Pn,i}} + (1 - \alpha) c_i^{I-1}, \quad i = 1, \dots, n_c, \quad (2.4)$$

where  $I$  is the current iteration and  $\alpha$  is the damping factor which is set to  $\alpha = 0.5$ . This is similar to what is done in [1], with the difference that the correction is based on the stress in the current iteration and the damping factor is constant. The change in  $c_i^I$  seems to tend towards zero as the optimization problem converges, therefore the damping factor has a negligible influence on the accuracy of the maximum stress approximation.

In order to obtain the stress correction factor for the current iteration the aggregated stress is first computed according to (2.2) (or (2.3)). Then, when the correction factor has been computed, it is recomputed as

$$\tilde{\sigma}_i^{Pn} := c_i^I \tilde{\sigma}_i^{Pn}, \quad i = 1, \dots, n_c.$$

## 2.4 Sensitivity Analysis

The stress state in Gauss point  $\mathbf{a}$  is given by

$$\boldsymbol{\sigma}_a = \mathbf{C} \mathbf{B}_a \mathbf{u}(\boldsymbol{\rho}(\mathbf{x})) \rho_e^q(\mathbf{x}).$$

Hence, the derivative of the stress state w.r.t. design variable  $x_j$  is given by

$$\frac{\partial \boldsymbol{\sigma}_a}{\partial x_j} = \sum_{i=1}^{n_{el}} \left( \frac{\partial \boldsymbol{\sigma}_a}{\partial \mathbf{u}} \right)^T \frac{\partial \mathbf{u}}{\partial \rho_i} \frac{\partial \rho_i}{\partial x_j} + \frac{\partial \boldsymbol{\sigma}_a}{\partial \rho_e} \frac{\partial \rho_e}{\partial x_j}, \quad (\text{no sum over } e).$$

The derivative of the displacement vector is obtained from the state equation

$$\mathbf{K} \mathbf{u} = \mathbf{F} \Rightarrow \sum_{i=1}^{n_{el}} \frac{\partial \mathbf{u}}{\partial \rho_i} \frac{\partial \rho_i}{\partial x_j} = -\mathbf{K}^{-1} \sum_{i=1}^{n_{el}} \frac{\partial \mathbf{K}}{\partial \rho_i} \frac{\partial \rho_i}{\partial x_j} \mathbf{u}.$$

This gives

$$\frac{\partial \boldsymbol{\sigma}_a}{\partial x_j} = \mathbf{C} \mathbf{B}_a \mathbf{u} q \rho_e^{q-1} \frac{\partial \rho_e}{\partial x_j} - \mathbf{C} \mathbf{B}_a \rho_e^q \mathbf{K}^{-1} \sum_{i=1}^{n_{el}} \frac{\partial \mathbf{K}}{\partial \rho_i} \frac{\partial \rho_i}{\partial x_j} \mathbf{u}$$

The derivative of the equivalent stress measure w.r.t. design variable  $x_j$  is given by

$$\begin{aligned} \frac{\partial \tilde{\sigma}_a}{\partial x_j} &= \left( \frac{\partial \tilde{\sigma}_a}{\partial \boldsymbol{\sigma}_a} \right)^T \frac{\partial \boldsymbol{\sigma}_a}{\partial x_j} = \\ &= \left( \frac{\partial \tilde{\sigma}_a}{\partial \boldsymbol{\sigma}_a} \right)^T \left( \mathbf{C} \mathbf{B}_a \mathbf{u} q \rho_e^{q-1} \frac{\partial \rho_e}{\partial x_j} - \mathbf{C} \mathbf{B}_a \rho_e^q \mathbf{K}^{-1} \sum_{i=1}^{n_{el}} \frac{\partial \mathbf{K}}{\partial \rho_i} \frac{\partial \rho_i}{\partial x_j} \mathbf{u} \right) \end{aligned}$$

The derivative of the aggregated stress measure  $\tilde{\sigma}_c^{Pn}$  for cluster  $c$  w.r.t. the equivalent stress measure in stress evaluation point  $\mathbf{a}$  reads

$$\frac{\partial \tilde{\sigma}_c^{Pn}}{\partial \tilde{\sigma}_a} = c_c^I \left( \sum_{i=1}^{n_{a,c}} \tilde{\sigma}_i^P \right)^{\frac{1}{P}-1} \tilde{\sigma}_a^{P-1},$$

where  $n_{a,c}$  is the number of stress evaluation points in cluster  $c$  and the  $P$ -norm stress aggregation is used. The derivative of the aggregated stress measure with respect to design variable  $x_j$  reads

$$\frac{\partial \tilde{\sigma}_c^{Pn}}{\partial x_j} = \sum_{a=1}^{n_{a,c}} \frac{\partial \tilde{\sigma}_c^{Pn}}{\partial \tilde{\sigma}_a} \left( \frac{\partial \tilde{\sigma}_a}{\partial \boldsymbol{\sigma}_a} \right)^T \frac{\partial \boldsymbol{\sigma}_a}{\partial x_j} =$$

$$\begin{aligned}
&= \sum_{a=1}^{n_{a,c}} \frac{\partial \tilde{\sigma}_c^{pn}}{\partial \tilde{\sigma}_a} \left( \frac{\partial \tilde{\sigma}_a}{\partial \sigma_a} \right)^T \left( \mathbf{CB}_a \mathbf{u} q \rho_e^{q-1} \frac{\partial \rho_e}{\partial x_j} - \mathbf{CB}_a \rho_e^q \mathbf{K}^{-1} \sum_{i=1}^{n_{el}} \frac{\partial \mathbf{K}}{\partial \rho_i} \frac{\partial \rho_i}{\partial x_j} \mathbf{u} \right) = \\
&= \sum_{a=1}^{n_{a,c}} \frac{\partial \tilde{\sigma}_c^{pn}}{\partial \tilde{\sigma}_a} \left( \frac{\partial \tilde{\sigma}_a}{\partial \sigma_a} \right)^T \mathbf{CB}_a \mathbf{u} q \rho_e^{q-1} \frac{\partial \rho_e}{\partial x_j} - \sum_{a=1}^{n_{a,c}} \frac{\partial \tilde{\sigma}_c^{pn}}{\partial \tilde{\sigma}_a} \left( \frac{\partial \tilde{\sigma}_a}{\partial \sigma_a} \right)^T \mathbf{CB}_a \rho_e^q \mathbf{K}^{-1} \sum_{i=1}^{n_{el}} \frac{\partial \mathbf{K}}{\partial \rho_i} \frac{\partial \rho_i}{\partial x_j} \mathbf{u}
\end{aligned}$$

The adjoint variable  $\lambda_c$  for cluster  $c$  is defined as

$$\lambda_c^T = \sum_{a=1}^{n_{a,c}} \frac{\partial \tilde{\sigma}_c^{pn}}{\partial \tilde{\sigma}_a} \left( \frac{\partial \tilde{\sigma}_a}{\partial \sigma_a} \right)^T \mathbf{CB}_a \mathbf{K}^{-1} \rho_e^q \quad (2.5)$$

$$\Leftrightarrow$$

$$\mathbf{K} \lambda_c = \sum_{a=1}^{n_{a,c}} \frac{\partial \tilde{\sigma}_c^{pn}}{\partial \tilde{\sigma}_a} \mathbf{B}_a^T \mathbf{C}^T \frac{\partial \tilde{\sigma}_a}{\partial \sigma_a} \rho_e^q$$

Solving for  $\lambda_c$  and reinserting gives

$$\frac{\partial \tilde{\sigma}_c^{pn}}{\partial x_j} = \sum_{a=1}^{n_{a,c}} \left( \frac{\partial \tilde{\sigma}_c^{pn}}{\partial \tilde{\sigma}_a} \left( \frac{\partial \tilde{\sigma}_a}{\partial \sigma_a} \right)^T \mathbf{CB}_a \mathbf{u} q \rho_e^{q-1} \frac{\partial \rho_e}{\partial x_j} \right) - \lambda_c^T \sum_{i=1}^{n_{el}} \frac{\partial \mathbf{K}}{\partial \rho_i} \frac{\partial \rho_i}{\partial x_j} \mathbf{u}, \quad (2.6)$$

The only explicit dependence on  $x_j$  in (2.6) comes from the derivative of the physical variables w.r.t. the design variables  $\partial \rho_e / \partial x_j$ . The physical variables  $\rho$  are related to the design variables  $\mathbf{x}$  through the filter matrix  $\mathbf{H}$  as

$$\rho(\mathbf{x}) = \mathbf{H} \mathbf{x},$$

hence, the derivatives are

$$\frac{\partial \rho_e}{\partial x_j} = H_{ej}.$$

The derivative of the stiffness matrix  $\mathbf{K}$  w.r.t. design variable  $x_j$  now reads

$$\sum_{i=1}^{n_{el}} \frac{\partial \mathbf{K}}{\partial \rho_i} \frac{\partial \rho_i}{\partial x_j} = \sum_{i=1}^{n_{el}} \mathbf{A}_i (p \rho_i^{p-1} \mathbf{k}_i^0) \mathbf{A}_i^T H_{ij},$$

where  $\mathbf{A}_i$  is the connectivity matrix and  $\mathbf{k}_i^0$  the stiffness matrix for element  $i$ . The second term in (2.6) can now be written as

$$\lambda_c^T \sum_{i=1}^{n_{el}} \frac{\partial \mathbf{K}}{\partial \rho_i} \frac{\partial \rho_i}{\partial x_j} \mathbf{u} = \lambda_c^T \left( \sum_{i=1}^{n_{el}} \mathbf{A}_i (p \rho_i^{p-1} \mathbf{k}_i^0) \mathbf{A}_i^T \right) \mathbf{u} H_{ij}.$$

The above expression can be rewritten in terms of the a local adjoint variable  $\lambda_{c,i}$  containing the elements of  $\lambda_c$  associated to the global degrees of freedom of element  $i$  and the local displacement vectors  $\mathbf{u}_i, i = 1, \dots, n_{el}$  as

$$\lambda_c^T \left( \sum_{i=1}^{n_{el}} A_i (p \rho_i^{p-1} k_i^0) A_i^T \right) u = \sum_{i=1}^{n_{el}} \lambda_{c,i}^T (p \rho_i^{p-1} k_i^0) u_i.$$

The column vector(s)  $\psi_c \in \mathbb{R}^{n_{el}}$  is defined such that

$$\psi_{c,i} = \lambda_{c,i}^T (p \rho_i^{p-1} k_i^0) u_i.$$

Hence, the second term of (2.6) becomes

$$\lambda_c^T \sum_{i=1}^{n_{el}} \frac{\partial K}{\partial \rho_i} \frac{\partial \rho_i}{\partial x_j} u = \psi_c^T H_j$$

where  $H_j$  is column  $j$  of  $H$ . Similarly, the first term in (2.6) can be written as

$$\sum_{a=1}^{n_{a,c}} \left( \frac{\partial \tilde{\sigma}_c^{pn}}{\partial \tilde{\sigma}_a} \left( \frac{\partial \tilde{\sigma}_a}{\partial \sigma_a} \right)^T C B_a u q \rho_s^{q-1} \frac{\partial \rho_s}{\partial x_j} \right) = \sum_{a=1}^{n_{a,c}} \left( \frac{\partial \tilde{\sigma}_c^{pn}}{\partial \tilde{\sigma}_a} \left( \frac{\partial \tilde{\sigma}_a}{\partial \sigma_a} \right)^T C b_a u_s q \rho_s^{q-1} H_{sj} \right)$$

where  $b_a$  is the local strain displacement matrix for stress evaluation point  $a$ . The column vector(s)  $\phi_c \in \mathbb{R}^{n_{el}}$  is defined such that

$$\phi_{c,i} = \sum_{a=1}^{n_{a,c}} \left( \frac{\partial \tilde{\sigma}_c^{pn}}{\partial \tilde{\sigma}_a} \left( \frac{\partial \tilde{\sigma}_a}{\partial \sigma_a} \right)^T C b_a u_s q \rho_s^{q-1} \right) \quad (2.7)$$

where  $n_{a,i}$  is the number of stress evaluation points in element  $i$ . The first term in (2.6) now becomes

$$\sum_{a=1}^{n_{a,c}} \left( \frac{\partial \tilde{\sigma}_c^{pn}}{\partial \tilde{\sigma}_a} \left( \frac{\partial \tilde{\sigma}_a}{\partial \sigma_a} \right)^T C B_a u q \rho_s^{q-1} \frac{\partial \rho_s}{\partial x_j} \right) = \phi_c^T H_j.$$

The derivative of the aggregated stress measure w.r.t. design variable  $x_j$  can hence be obtained as

$$\frac{\partial \tilde{\sigma}_c^{pn}}{\partial x_j} = \phi_c^T H_j - \psi_c^T H_j = (\phi_c - \psi_c)^T H_j. \quad (2.8)$$

The expression in (2.8) is valid for any equivalent stress measure, the only difference is the expression for the derivative of the equivalent stress measure w.r.t. the stress state which appears in the definition of the adjoint variables in (2.5) and the definition of  $\phi$  in (2.7).

For the von Mises equivalent stress, these derivatives are given by

$$\frac{\partial \tilde{\sigma}_a}{\partial \sigma_a} = \frac{\partial \sigma_a^{vM}}{\partial \sigma_a} = \frac{1}{2\sigma_a^{vM}} \begin{bmatrix} 2\sigma_{ax} - \sigma_{ay} - \sigma_{az} \\ 2\sigma_{ay} - \sigma_{ax} - \sigma_{az} \\ 2\sigma_{az} - \sigma_{ax} - \sigma_{ay} \\ 6\tau_{axy} \\ 6\tau_{ayz} \\ 6\tau_{azx} \end{bmatrix}.$$

And for the maximum principle stress, the associated derivatives are

$$\frac{\partial \tilde{\sigma}_a}{\partial \sigma_a} = \frac{\partial \sigma_a^1}{\partial \sigma_a} = \begin{bmatrix} \phi_1^2 \\ \phi_2^2 \\ \phi_3^2 \\ 2\phi_1\phi_2 \\ 2\phi_2\phi_3 \\ 2\phi_1\phi_3 \end{bmatrix},$$

where  $\phi = [\phi_1 \ \phi_2 \ \phi_3]^T$  is the (normalized) eigenvector of the stress matrix associated to the largest principle stress [2].

## 2.5 Discussion

The implementation of the stress constraints in Trinitas has been extensively tested by the author using several examples in 2D and 3D and the implementation of the sensitivity analysis for the von Mises equivalent stress and the maximum principle stress have been verified using finite differences. This section gives an account of some of the authors experiences and observations during the testing of the implementation.

### 2.5.1 Stress Clusters

As mentioned in [5] the use of stress clusters is not strictly necessary in order to achieve a good approximation of the maximum stress when the stress correction is used. However, using clusters generally gives better results with moderate values of  $P$  and more “aggressive” settings can be used in the optimization solver. Figure 1 shows a comparison using the L-Beam example with  $P = 6$  and  $n_c \in \{1, 4, 8\}$ . The mass is minimized using a von Mises stress constraint.

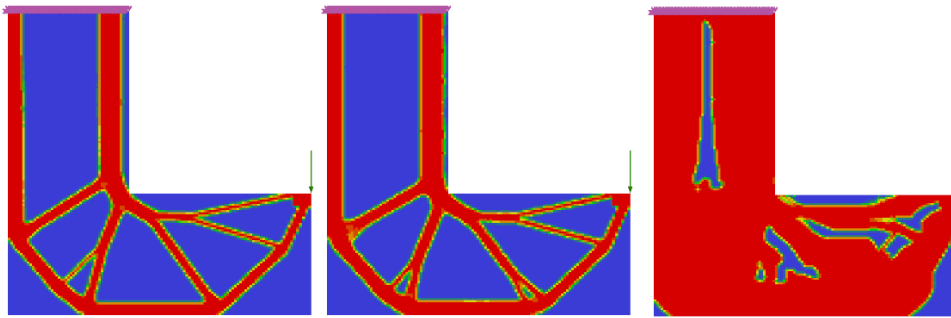


FIGURE 1 – RESULTS FOR L-BEAM USING DIFFERENT  $n_c$ ,  $m$  IS THE RELATIVE MASS.  
LEFT:  $n_c = 8$ ,  $m = 1$ . MIDDLE:  $n_c = 4$ ,  $m = 1.08$ . RIGHT:  $n_c = 1$ ,  $m = 2.81$ .

As seen in Figure 1 (Right) the optimization fails completely for this value of  $P$  when clusters are not used. Using  $P$  values this low is not recommended (even though it does work in this case), generally  $P \geq 8$  seems to give good results.



Even though using clusters makes the optimization problem seemingly simpler to solve they should be used moderately, especially for large problems with a large number of loadcases. Since each cluster is a separate constraint in the optimization problem the number of constraints can quickly become too large for the MMA (or GCMMA) algorithm to handle. As an example, the L-Beam in Figure 1 contains 11130 Q4 elements. Running 350 iterations with 1 cluster takes 56.12 seconds, 32 clusters takes 135.9 seconds and 64 clusters takes 278.4 seconds. A small part of the difference is due to the sensitivity computation since more clusters mean more adjoint systems to solve, however, this is negligible compared to the time consumed by the optimization solver. This problem is somewhat relieved by using a high reclustering frequency (low value of  $f_c$ ) since some of the constraints may become inactive. Using  $f_c \geq 10$  is however recommended since lower values of  $f_c$  may result in convergence issues.

Of the three different implemented clustering methods in Trinitas, the only one that should ever be used in practise is “distributed stress” (which is also the default method in Trinitas). The “element numbers” method is somewhat random and may or may not give good results. The “stress level” method generally gives poor results since all the largest stresses are contained in the same constraint. This method was evaluated using the  $P$ -norm as well as the  $P$ -mean aggregation functions and never works as good as the “distributed stress” method.

### 2.5.2 MMA Parameters

When stress constraints are used, the optimization problems become highly sensitive to the MMA parameters. Specifically the asymptote widening  $s_f$  and narrowing  $s_s$  coefficients.

If no clusters are used conservative values have to be specified, otherwise the optimization will simply fail and the result is modern art instead of an optimized structure. Typically  $s_f \approx 1.05$  and  $s_s \approx 0.6$  seems to work well for a single global stress constraint with  $P \in [10,12]$ . Unfortunately these parameters are also somewhat problem size dependent so what works well for 6,000 elements may not work so well for 600,000 elements.

If clusters are used (typically  $n_c \geq 8$  is recommended) the problems tend to be more stable and more aggressive parameters can be used. Typically  $s_f \approx 1.05$  and  $s_s \approx 0.85$  should be used for  $P = 8$  and  $n_c \geq 8$ . Using clusters also seem to relieve the problem size dependence of the MMA parameters. The previously specified values have been used successfully for problems of widely varying size and complexity, from 2D problems with 4,000 elements with a single loadcase to 3D problems with 500,000 elements and several load cases. Note that “successfully” in this context does not imply a low tolerance on the objective function value.

Perhaps MMA is not the most suitable optimization solver for these types of problems, a more modern and robust solver, e.g. IPOPT, may give better results.

## 3. Additive Manufacturing & Topology Optimization

Two different specific aspects of additive manufacturing (AM) and TO have been considered in the ADDMAN project so far. The first is how to deal with the anisotropic material properties which may result from the manufacturing process. And the second is manufacturing constraints for AM in order to limit or eliminate support structures when printing the optimized structures. Anisotropic material properties is covered extensively in [5] and is therefore omitted here.

### 3.1 Overhang Filter

There are several different approaches when it comes to limiting the need for support structures in TO optimized structures. The most promising approach was developed by Langelaar who uses a filtering technique in order to eliminate overhangs in the optimized structures [5].

In Langelaars approach an additional “blueprint” density field  $\rho^b$  is added to the formulation of the TO problem and the value of the physical densities  $\rho$  is given by

$$\rho_i = \min\{\rho_i^b, \max\{\rho \in \Theta_i\}\}, \quad (3.1)$$

where  $\Theta_i$  is the set of nearby finite elements in the AM build layer underneath element  $i$ , see Figure 2.

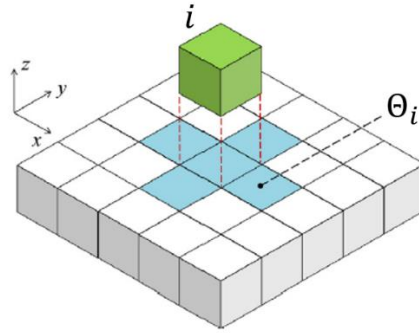


FIGURE 2 – ILLUSTRATION OF THE SET  $\Theta$ . FIGURE REPRODUCED FROM [5]

In order for (3.1) to be differentiable the min and max operators are approximated using the smooth functions

$$\min\{\rho_i^b, \hat{\rho}_i\} \approx \text{smin}\{\rho_i^b, \hat{\rho}_i\} = \frac{1}{2} \left( \rho_i^b + \hat{\rho}_i - \left( (\rho_i^b - \hat{\rho}_i)^2 + \epsilon \right)^{\frac{1}{2}} + \sqrt{\epsilon} \right), \quad (3.2)$$

where  $\epsilon$  is a small positive real number, and

$$\max\{\rho \in \Theta_i\} \approx \text{smax}\{\rho \in \Theta_i\} = \left( \sum_{j \in \Theta_i} \rho_j^P \right)^{\frac{1}{Q}} = \hat{\rho}_i, \quad (3.3)$$

where  $P$  and  $Q$  are positive real numbers. Langelaar suggests the following values for these parameters

$$P = 40, \quad Q = P + \frac{\log n}{\log \rho_0}, \quad \epsilon = 10^{-3}$$

where  $n = 3$  for 2D problems,  $n = 5$  for 3D problems and  $\rho_0 = 0.5$ .

A drawback with Langelaars approach is that the finite element mesh has to be partitioned into layers in the build direction which limits its use for general unstructured meshes or meshes with varying element sizes. Hoffarth et. al. seem to get around this problem by defining the set  $\Theta$  as the elements contained in a conical volume underneath the element of interest [6]. The mathematical details are however scarce and it is unclear whether layers have to be defined or not.

### 3.1.1 Sequence Based AM Filter

The AM filter implemented in Trinitas is heavily based on the one by Langelaar. However no layers have to be defined and the method works well for general meshes and build directions. A “blueprint” density field is used and the physical densities are defined in the same way as in Langelaars method using (3.1) with the smooth approximations given by (3.2) and (3.3). Two sets of element sets are used, one for the filtering process,  $\Theta_{Fi}$ , and one for the sensitivity analysis,  $\Theta_{Si}$ . A conical volume is used to defined the elements in the sensitivity sets, see Figure 3.

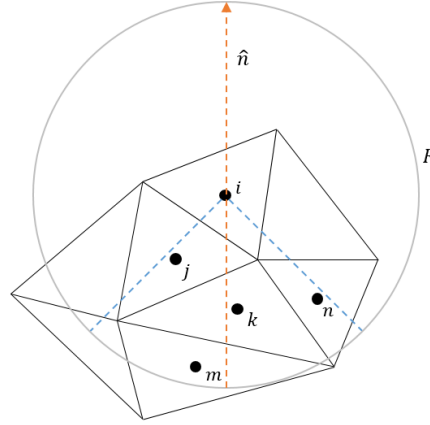


FIGURE 3 - CONICAL VOLUME USED TO DEFINED THE SETS  $\Theta_{Fi}$ .  
THE DOTS INDICATE THE CENTRE OF MASS OF THE ELEMENTS.

The filtering set for blueprint variable  $i$  is defined as

$$\Theta_{Fi} = \left\{ \rho_j : \|v_{ij}\| \leq R_c, \cos^{-1} \left( \frac{(-\hat{n} \cdot v_{ij})}{\|v_{ij}\|} \right) \leq \theta_{max} \right\}. \quad (3.4)$$

where  $v_{ij}$  is the position vector of the centre of mass of element  $j$  relative to element  $i$ ,  $R_c$  is the radius of the cone,  $\hat{n}$  is a unit vector in the build direction and  $\theta_{max}$  is the maximum allowed overhang angle. In the filtering process, the set  $\Theta_{Fi}$  replaces  $\Theta_i$  in (3.1).

Even though no layers are defined, the filter application (3.1) has to be done in a sequence going from the lowest to the highest element in the build direction. This sequence is obtained by projecting the centres of mass of all the elements onto the build direction and arranging them in order from lowest to highest. If two or more elements share the same height in the build direction, the ordering between them does not matter.

### 3.1.2 Sensitivity Analysis

The sensitivity set  $\Theta_{Si}$  is defined as the set of all physical variables with explicitly depend on blueprint variable  $i$  in (3.1), i.e. if  $j \in \Theta_{Fi}$  then  $i \in \Theta_{Dj}$ . The sensitivity analysis is performed in the opposite order compared to the application of the filter. For a given constraint or objective function  $f$ , adjoint variables  $\lambda_j$  are defined as

$$\lambda_j = \frac{\partial f}{\partial \rho_j} + \sum_{i \in \Theta_{Sj}} \lambda_i \frac{\partial \rho_i}{\partial \rho_j}, \quad (3.5)$$

where  $\Theta_{sj} = \emptyset$  if element  $j$  has no higher neighbours, and

$$\frac{\partial \rho_i}{\partial \rho_j} = \frac{\partial}{\partial \rho_j} (\text{smin}\{\rho_i^b, \hat{\rho}_i\}). \quad (3.6)$$

The sensitivities for the function of interest w.r.t. the blueprint variables is the obtained as

$$\frac{\partial f}{\partial \rho_j^b} = \lambda_i \frac{\partial \rho_i}{\partial \rho_j^b},$$

where

$$\frac{\partial \rho_i}{\partial \rho_i^b} = \frac{\partial}{\partial \rho_i^b} (\text{smin}\{\rho_i^b, \hat{\rho}_i\}). \quad (3.7)$$

Note that the sensitivities in (3.6) and (3.7) do not depend on the function of interest and therefore only has to be computed once. Furthermore, the adjoint variables for different objective and constraint functions can be computed in parallel for large problems with a large number of constraints, e.g. stress constrained problems with a large number of clusters and loadcases.

### 3.1.3 Numerical Example

The AM filter is evaluated using an industrially representative 3D geometry with a structured mesh of varying element sizes. Figure 4 shows the design domain (light brown), the functional areas (blue) and the boundary extension used to achieve a consistent filtering of internal and external boundaries (green). The build direction is defined to be parallel to the axis of the four vertical holes.

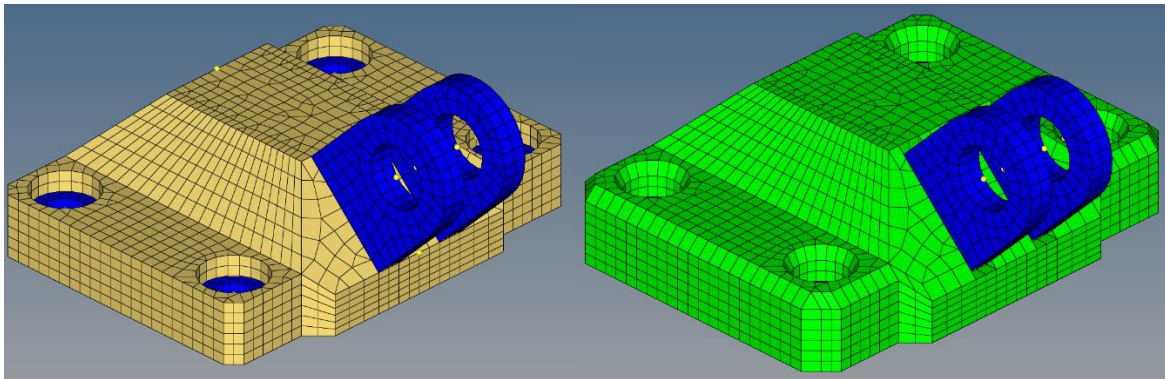


FIGURE 4 – EXAMPLE PROBLEM FOR EVALUATION OF AM FILTER.

The mass is minimized with a constraint on the maximum von Mises stress using three loadcases. The discretization used in the optimization is shown in Figure 5 and contains a mix of 459,872 1<sup>st</sup> order brick, wedge and tetrahedral elements. The maximum overhang angle is set to  $\theta_{max} = 45^\circ$ .

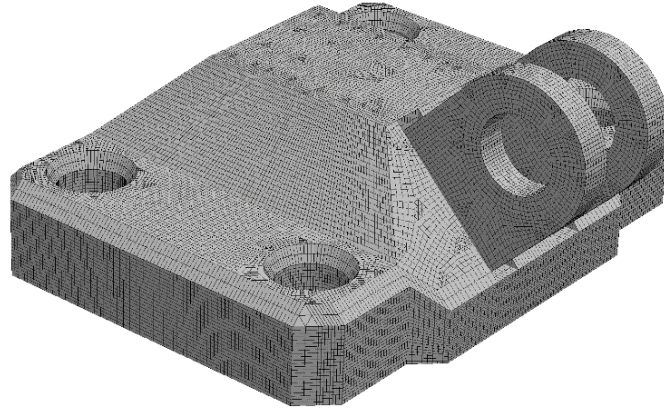


FIGURE 5 – DISCRETIZATION USED IN THE TOPOLOGY OPTIMIZATION.

Figure 6 shows the results from the topology optimization. As seen in the figure there are no horizontal overhangs in the optimized structure.

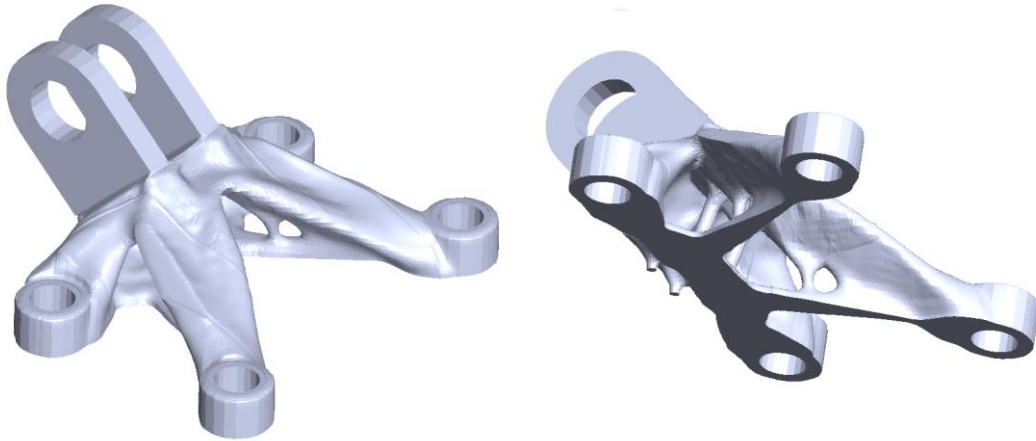


FIGURE 6 – RESULTS FROM TOPOLOGY OPTIMIZATION USING AM FILTER

### 3.1.4 Discussion

In this section a few of the issues and nuances of the method is discussed, as well as some extensions, modifications and alternative use cases.

#### 3.1.4.1 Filter Parameters

The behaviour of the AM filter depends to a large extent on the values of the parameters  $P$ ,  $Q$  and  $\epsilon$ . The reason why the conventional  $P$ -norm is not used is that it overestimates the maximum value of the approximated set which may lead to gradual build-up of material from void. The specific value of  $Q$  is motivated by the number of lower neighbours for 2D and 3D problems which is fixed to 3 in 2D problems and 5 in 3D problems in Langelaars formulation [7] [5]. In the modified formulation the number of lower neighbours depend on the mesh, chosen radius and overhang angle. Therefore a suitable value is hard to specify. One option, which was chosen for the implementation is to set

$$n = \max\{|\Theta_{Fi}|\},$$

i.e.  $n$  is set to the largest cardinality of the filtering sets  $\Theta_{Fi}$ . Figure 7 shows an MBB-Beam optimized for maximum stiffness with all parameters equal except for the value of  $Q$ ,  $\rho_0 = 0.5$ .

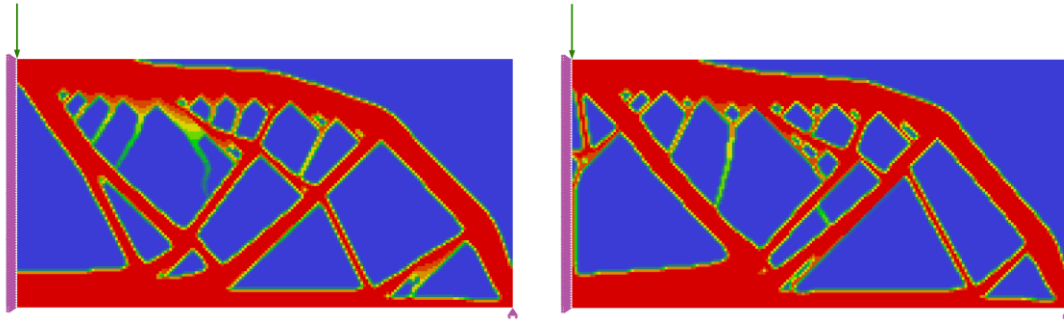


FIGURE 7 – MBB-BEAM OPTIMIZED FOR MAXIMUM STIFFNESS WITH AN OVERHANG CONSTRAINT.  
LEFT:  $Q = P = 40$ . RIGHT:  $P = 40, Q = P + \text{LOG}(\text{MAX}\{|\Theta_{Fi}|\}) / \text{LOG } \rho_0$ .

Another option is to use the conventional  $P$ -norm with larger values of  $P$ . However, for the values of  $P$  necessary to give a good approximation of the maximum, numerical issues occur and the problem becomes difficult to solve. One may also consider using correction factors similar to what is done for stress constraints, however, since the approximated functions don't tend towards any particular value this approach does not work in this case.

The issue of material build-up from void does not seem to be as pronounced for 3D problems as it is in 2D since one more spatial dimension is available to fulfil the overhang restriction making the problem in some sense easier. And since 2D problems are exclusively used for evaluation purposes this issue may not require any further attention.

Another parameter that needs consideration is the radius of the filter cone,  $R_C$ . Ideally the filtering set  $\Theta_{Si}$  for a particular element should only contain the adjacent elements underneath. However, since the elements may vary in shape and size a suitable value for  $R_C$  may be hard to specify. One option is to set the cone radius equal to the density filter radius,  $R$ , however, if a small density filter radius is used the filtering set may only contain a single element, effectively restricting the overhang angle to 0, see Figure 8 (Left). In this case the cone radius should be larger than the density filter radius, see Figure 8 (Right).

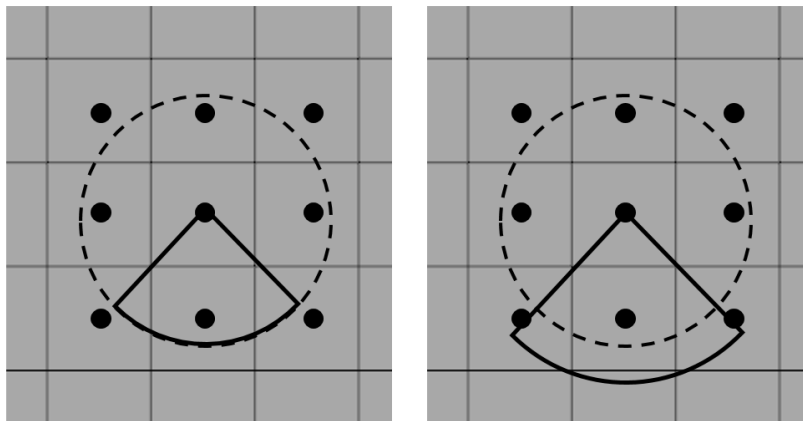


FIGURE 8 – AM FILTER CONE RADIUS. LEFT: CONE RADIUS EQUAL TO DENSITY FILTER RADIUS.  
RIGHT: CONE RADIUS LARGER THAN DENSITY FILTER RADIUS.



Using a large cone angle may however result in other issues. If several “layers” of elements are contained in the cone, the optimized structure may contain small void patches in the supporting material since the overhang restriction is fulfilled by elements a few “layers” beneath, see Figure 9.

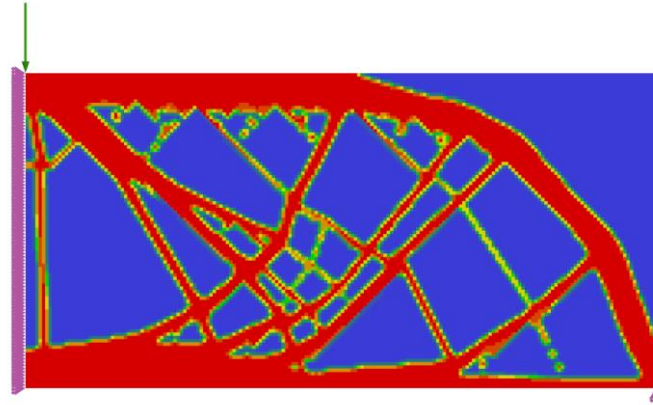


FIGURE 9 – MBB-BEAM WITH  $R_c = 3R$ .

Choosing a suitable cone radius requires consideration of the chosen density filter radius, the discretization used and possibly some trial and error. Another consideration is the orientation of the mesh w.r.t. the chosen build direction, a cone radius which works well for a certain direction may not work equally well for another, see Figure 10.

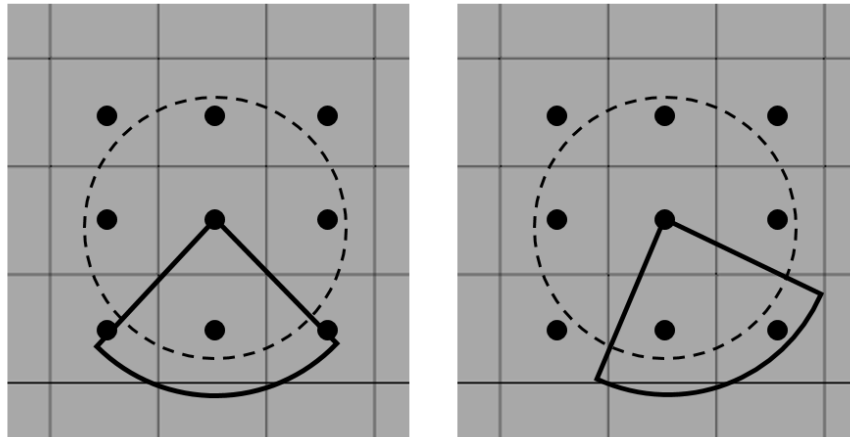


FIGURE 10 – DIFFERENT BUILD ORIENTATIONS FOR A STRUCTURED MESH.

Perhaps there is a better definition of the filter region than the one in (3.4), e.g. see Figure 11. An issue with the one used at present is that for a structured mesh with the build direction parallel to the element sides and a maximum overhang angle of  $45^\circ$ , the element centres lie on the surface of the cone which means that they may or may not be included in  $\Theta_{Fi}$ , see Figure 10 (Left). Therefore, the maximum overhang angle has to be set slightly larger than the desired in some cases. The shape of the filter region only determines the elements of  $\Theta_{Fi}$  and  $\Theta_{Si}$  and can be modified without any other changes to the implementation.

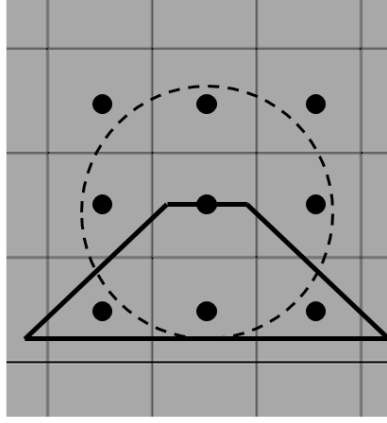


FIGURE 11 – DIFFERENT SHAPE OF FILTER REGION.

#### 4. Boundary Extension

Using the standard linear density filter, the physical design variables are given by

$$\rho_i = \sum_{s \in \Omega_R} W_{is} x_s, \quad (4.1)$$

where  $\Omega_R$  is the filter region and the weights  $W_{is}$  are given by

$$W_{is} = \frac{\max(R - \|v_{is}\|, 0)}{\sum_{j \in \Omega_R} \max(R - \|v_{ij}\|, 0)} = \frac{\omega_{is}}{\phi_i}, \quad (4.2)$$

where  $v_{pk}$  is the position vector of element  $p$  w.r.t. element  $k$ . From (4.2) it follows that

$$\sum_{s \in \Omega} W_{is} = 1. \quad (4.3)$$

Now consider an inner boundary  $\Gamma^I$  and an outer boundary  $\Gamma^O$ , where the outer boundary is also the boundary of the design space, see Figure 12. For simplicity we say that the design variables have the value 1 in the region  $\Omega$  and 0 elsewhere, hence  $\Gamma^I$  and  $\Gamma^O$  are both external boundaries to the structure and should be treated equally by the filter.



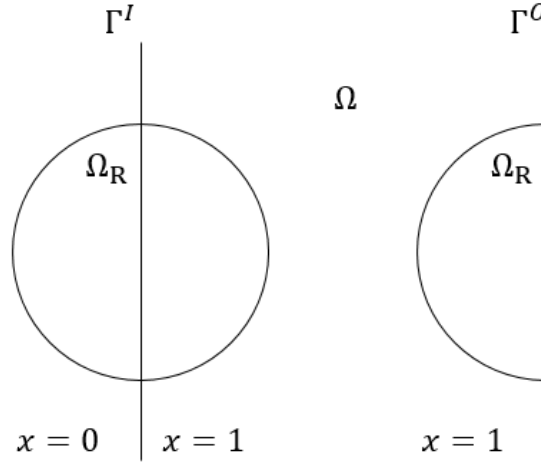


FIGURE 12 – FILTER OPERATION AT AN INTERNAL AND EXTERNAL BOUNDARY.

Since  $x = 0$  outside  $\Omega$  it holds that

$$\rho_i^I = \sum_{e \in \Omega_R \cap \Omega} W_{ie}^I x_e, \quad \forall \rho \text{ on } \Gamma^I,$$

and

$$\rho_i^O = \sum_{e \in \Omega_R \cap \Omega} W_{ie}^O x_e, \quad \forall \rho \text{ on } \Gamma^O.$$

However, the boundaries are not treated equally since

$$\phi_i^I = \sum_{j \in \Omega_R} \max(R - \|v_{ij}\|, 0) \geq \sum_{j \in \Omega_R \cap \Omega} \max(R - \|v_{ij}\|, 0) = \phi_i^O,$$

and therefore

$$W_{ie}^I \leq W_{ie}^O, \quad \forall e \in \Omega_R \cap \Omega.$$

Since  $x = 1 \in \Omega_R \cap \Omega$  it follows that  $\rho_i^O = x_i$  on  $\Gamma^O$  and  $\rho_i^O \leq x_i$  on  $\Gamma^I$ . This effectively makes the length scale control different for external and internal boundaries. It also makes the external boundaries preferable in the optimization problems since the filter has a smaller effect there.

For a structured mesh with equal sized elements there is a simple fix to this problem, namely letting

$$W_{ie} = \frac{\omega_{ie}}{\phi}, \quad \phi = \max \phi_i. \quad (4.4)$$

This would result in external and internal boundaries being treated in the same way, assuming the lower bound on the design variables is small. For a general discretization with elements of different shapes and sizes using the definition of the weights in (4.4) is not ideal. For a density variable with  $\Omega_R \subset \Omega_D$ , where  $\Omega_D$  is the design space, (4.3) must hold. This may be violated if (4.4) is used for general discretizations.

Another option is to extend the finite element mesh with void elements outside the design space, which was proposed in [9]. These elements are assigned pseudo design variables at the lower bound and used in the filter operation to represent the void outside the design space, see Figure 13.

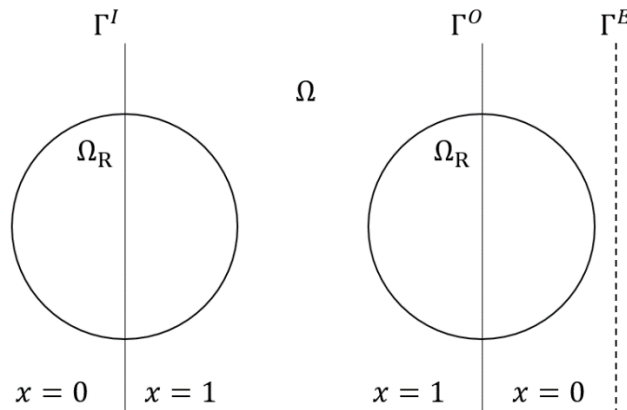


FIGURE 13 – BOUNDARY EXTENSION.

The boundary extension should be at least one filter radius in order to achieve an equal treatment of internal and external boundaries. Since the boundary extension reduces the density of the elements on the external boundaries it should not be used in the vicinity of boundary conditions.

Figure 14 shows a comparison of the L-beam optimized for minimum mass with a stress constraint with and without the boundary extension applied. Some minor differences can be seen in the optimized structures. Most noticeable is the smoother transition in the left vertical member as it leaves the outer boundary.

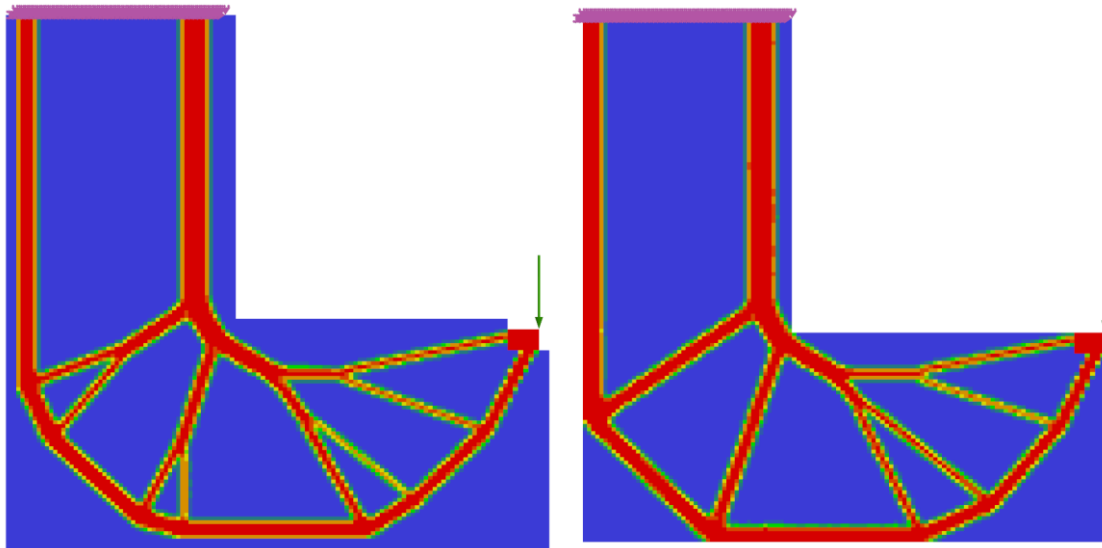


FIGURE 14 – L-BEAM WITH AND WITHOUT BOUNDARY EXTENSION.

Figure 15 shows a comparison of the bracket from Section 3.2.3 with and without the boundary extension applied. In this case the difference is more pronounced. The use of the boundary extension leads to a smoother structure without the sharp transitions as the material “sticks” to the outer boundaries.

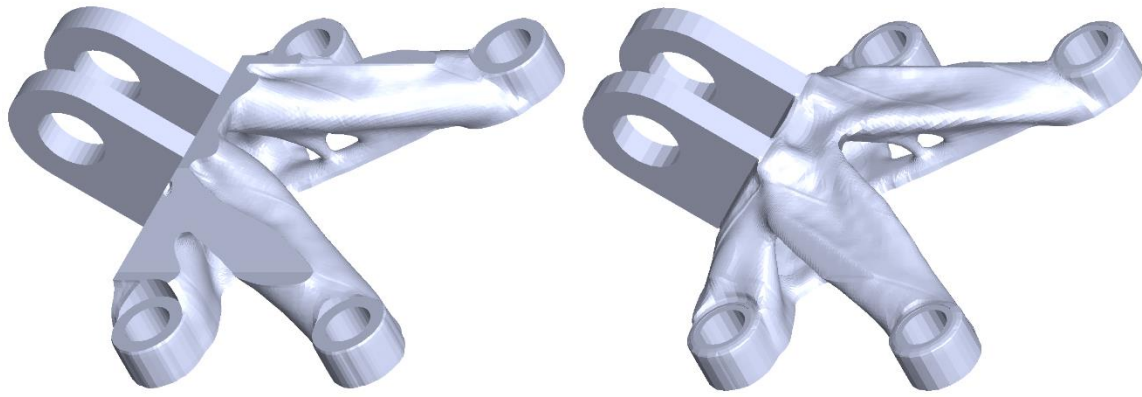


FIGURE 15 – BRACKET WITH AND WITHOUT BOUNDARY EXTENSION.

## 5. References

- [1] C. Le, J. Norato, T. Bruns, C. Ha and D. Tortorelli, “Stress-based topology optimization for continua,” *Structural and Multidisciplinary Optimization*, no. 41, pp. 605-620, 2010.
- [2] E. Holmberg, “Topology optimization considering stress, fatigue and load uncertainties,” Linköping University, Linköping, 2015.
- [3] M. Bruggi, “On an alternative approach to stress constraints relaxation in topology optimization,” *Structural and Multidisciplinary Optimization*, no. 36, pp. 125-141, 2008.
- [4] “Fortran-parallel-sort,” [Online]. Available: <https://github.com/cphyc/Fortran-parallel-sort>.
- [5] H. A. Grundström, “Topology Optimization for Additive Manufacturing Considering Stress and Anisotropy,” Linköping University, Linköping, 2017.
- [6] M. Langelaar, “Topology Optimization of 3D self-supporting structures for additive manufacturing,” *Additive Manufacturing*, no. 12, pp. 60-70, 2016.
- [7] M. Hoffarth, N. Gerzen and C. Pedersen, “ALM Overhang Constraint in Topology Optimization for Industrial Applications,” in *12th World Congress on Structural and Multidisciplinary Optimization*, Braunschweig, Germany, 2016.
- [8] M. Langelaar, “An additive manufacturing filter for topology optimization of print-ready designs,” *Structural and multidisciplinary optimization*, 2015.

- [9] E. Holmberg, B. Torstefelt and A. Klarbring, "Global and clustered approaches for stress constrained topology optimization and deactivation of design variables," in *10th World Congress on Structural and Multidisciplinary Optimization*, Orlando, Florida, USA, 2013.